

Differentially private inference framework of Riemannian manifold data

Yangdi Jiang ^{*,‡}, Xiaotian Chang^{*,‡}, and Qirui Hu^{†,§}

Abstract

We propose a novel and systematic differentially private (DP) inference framework for non-Euclidean data. First, we design two types of DP mechanisms for the Fréchet mean and variance with i.i.d. Riemannian manifold-valued data, tailored to different geometric structures and accompanied by analytic privacy budgets calibrated to the geometry of the underlying manifold. Second, we establish the consistency and central limit theorems (CLTs) of the proposed DP estimators, enabling a suite of statistical inference procedures under privacy protection. Furthermore, we provide comprehensive implementation guidelines and feasible procedures, including consistent DP estimators of the asymptotic variance in the CLTs. Extensive numerical experiments support the proposed methodologies. Finally, we demonstrate the effectiveness of our approach on real-world medical image and sociological datasets lying on two representative manifolds.

Keywords: Differential privacy, Fréchet analysis, Manifold-valued data, Statistical inference

*School of Physical and Mathematical Sciences, Nanyang Technological University

†School of Statistics and Data Science, Shanghai University of Finance and Economics

‡Co-first authors. These authors contributed equally to this work.

§Corresponding author: huqirui@mail.shufe.edu.cn

1 Introduction

As computing technology advances, the data collected have become increasingly complex. Many such complex datasets reside in nontraditional spaces, namely Riemannian manifolds. One of the most prominent examples in statistics is the space of symmetric positive definite matrices (SPDMs), which frequently arises in imaging analysis, where it models the covariance matrices of features extracted from images [Tuzel et al., 2006]. In particular, SPDMs are widely used to represent the covariance of water molecule diffusion in Diffusion Tensor Imaging (DTI) [Pennec et al., 2019, Basser et al., 1994]. Another commonly studied manifold is the (hyper)sphere, which forms the foundation of directional statistics [Mardia and Jupp, 2000, Fisher et al., 1987]. Directional statistics deal with data representing directions, that is, unit vectors. For directions in the plane, the data are circular, while for directions in three-dimensional space, the data are spherical. Figures 1 and 2 illustrate examples of sociological and medical imaging data, respectively, which differ substantially from Euclidean data; see Section 6 for further details.

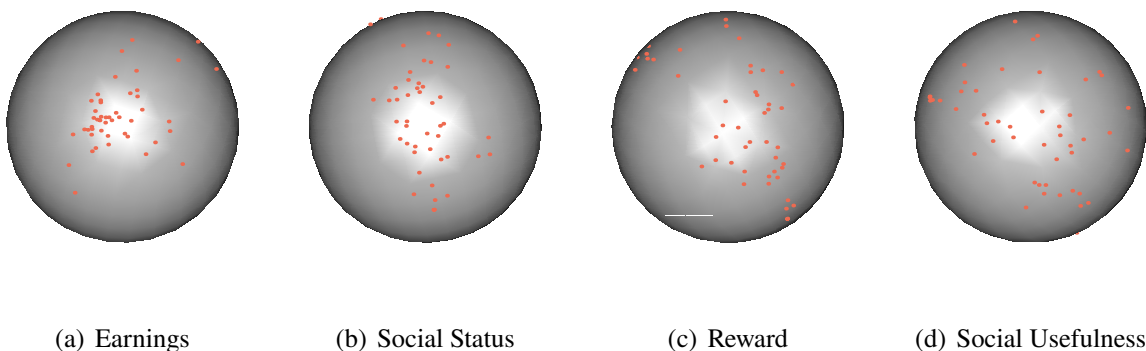


Figure 1: The occupational judgment data based on 4 different criteria [Fisher et al., 1987, Page 301].

On the other hand, the non-Euclidean datasets presented in Section 6 are closely

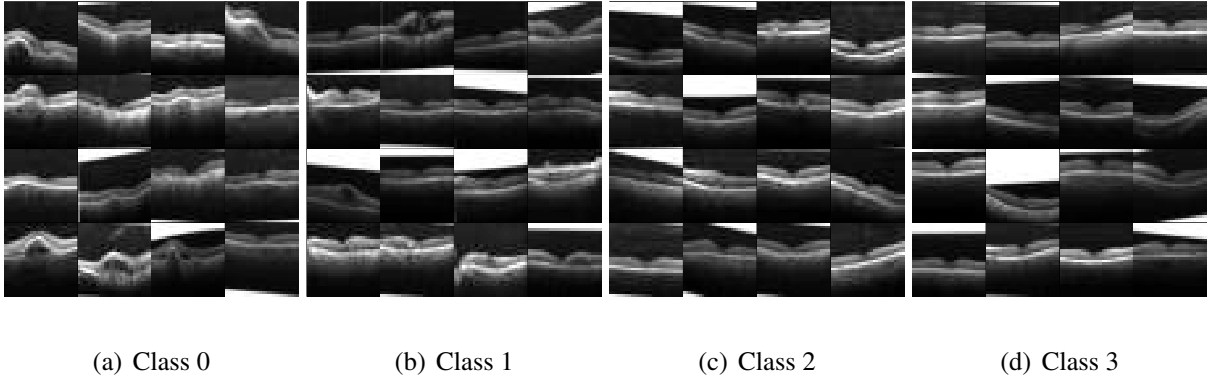


Figure 2: The first 16 images from each of 4 diagnosis categories in OCTMNIST dataset [Yang et al., 2021a,b].

linked to personal information, raising concerns about potential privacy leakage. Such concerns also arise in many other scenarios: datasets from government agencies, private organizations, and research institutions cannot be publicly shared without strong anonymization or protection measures. This limitation restricts the availability of high-quality data for interdisciplinary research across fields such as healthcare, social sciences, and artificial intelligence. To address these challenges, differential privacy (DP) was introduced by Dwork et al. [2006] as a formal framework for privacy-preserving data analysis. However, developing a DP framework for manifold-valued data remains largely unexplored due to the analytical complexity introduced by curvature. Existing studies primarily focus on Euclidean data analysis under DP, e.g., Liu et al. [2023, 2024], whereas privacy-protected mechanisms for non-Euclidean data and further statistical inference on manifolds with privacy guarantees have made very limited progress.

In this paper, we consider the inference problem for the Fréchet mean and variance of a collection of confidential data defined on a d -dimensional manifold \mathcal{M} under the DP framework. Specifically, the data curator has access to a confidential dataset

consisting of i.i.d. observations $D = \{X_1, \dots, X_n \in \mathcal{M}\}$ drawn from some unknown probability measure \mathbb{P} on \mathcal{M} . Our primary goal is the estimation and inference of the population Fréchet mean η and the corresponding Fréchet variance V , with detailed definitions provided in Definition 1.

The Fréchet mean generalizes the notion of the Euclidean mean to abstract metric spaces. Similar to the Euclidean sample mean, a natural statistic to consider here is its sample version; see Definition 1. However, under DP constraints, one cannot directly access the sample Fréchet mean, but only its DP version. In Euclidean spaces, the DP sample mean is typically obtained by adding zero-mean random noise, where the concentration of the noise is controlled by the desired level of privacy protection, specified through the privacy budget parameters. In contrast, for manifold-valued data, such a DP mechanism does not automatically preserve the manifold constraint due to the absence of a vector space structure. Moreover, additional challenges arise when extending DP statistical inference to manifold-valued data.

Guided by the intrinsic geometry of Riemannian manifolds, a key contribution of this paper is that we consider two novel DP mechanisms: the Riemannian Gaussian (RG) for homogeneous manifolds with positive curvature (see Section S.1.3 in the supplementary material) and the Exponential-Wrapped Gaussian (EWG) for Hadamard manifolds. These two mechanisms cover many common non-Euclidean data settings, such as medical imaging data on the SPD manifold and sociological data on the sphere (see Section 6 for data applications). For homogeneous manifolds of positive curvature, we further establish an analytic relationship among sensitivity, Riemannian geometry, and the privacy budget, which generalizes the classical Euclidean result in \mathbb{R}^d and enables direct computation of the noise level from sensitivity.

This approach relaxes the restrictive constant-curvature assumption to the broader class of homogeneous positive-curvature manifolds and obviates the need to invert the privacy budget for a fixed noise level, eliminating additional MCMC or other numerical procedures required in prior work such as [Jiang et al. \[2023\]](#).

Furthermore, we provide a detailed asymptotic analysis of the proposed DP estimators. In particular, we prove \sqrt{n} -consistency and CLTs under additional higher-order DP noise, yielding valid DP inference for the Fréchet mean and variance, including the construction of confidence regions. We also study the effect of smeariness and derive the smeary asymptotics of the Fréchet mean, demonstrating slower convergence rates induced by geometric structure. We offer practical, comprehensive implementations of the DP inference procedures and propose consistent DP estimators for the corresponding asymptotic variances. To the best of our knowledge, this manuscript is the first to address the DP inference problem with novel privacy mechanisms and to provide a general, implementable inference framework for confidential manifold-valued data.

We conclude this introduction with a brief review of manifold-valued data inference, which can be broadly categorized into two main branches. The first branch focuses on statistical inference for data directly sampled from a manifold. Foundational work by [Bhattacharya and Patrangenaru \[2003, 2005\]](#) established the large-sample properties of sample means on manifolds, providing crucial building blocks for subsequent studies. Later, [Eltzner and Huckemann \[2019\]](#) introduced a CLT grounded in the notion of smeariness, extending the earlier theoretical framework. Beyond the analysis of sample means, additional manifold-related topics, including Fréchet variance analysis, Fréchet regression, and Fréchet change-point detection, have at-

tracted significant interest; see, for example, [Dubey and Müller \[2019\]](#), [Petersen and Müller \[2019\]](#), [Dubey and Müller \[2020a\]](#). More recent efforts seek to refine and generalize these models, such as robust and generalized Fréchet means [[Yang and Vemuri, 2020](#), [McCormack and Hoff, 2023](#), [Lee and Jung, 2025](#), [Blanchard and Jaffe, 2025](#)], enhanced regression frameworks [[Jeon et al., 2021](#), [Bhattacharjee et al., 2023](#), [Lin and Chen, 2024](#), [Zhang et al., 2024](#)], additional limit theory [[Chakraborty and Vemuri, 2019](#), [Evans and Jaffe, 2024](#), [Dubey et al., 2024](#)], and optimization methods on manifold [[Kasai et al., 2019](#), [Becigneul and Ganea, 2019](#), [Jordan et al., 2022](#), [Tripuraneni et al., 2018](#)].

The second branch deals with modeling functions on manifolds, exemplified by [Dubey and Müller \[2020b\]](#), [Lin and Yao \[2021\]](#), and [Shao et al. \[2022\]](#), which develop elegant inference methods and associated theoretical results for manifold-valued functions. It is worth noting that, to the best of our knowledge, none of the aforementioned studies provides an inference theory with explicit privacy protections.

The paper is organized as follows. In [Section 2](#), we briefly introduce background on Riemannian manifolds and the DP framework on manifolds. [Section 3](#) presents the methodology and asymptotic results. Implementation details are provided in [Section 4](#). Numerical experiments and real data applications are given in [Sections 5](#) and [6](#), respectively. Additional background on Riemannian manifolds, the introduction to two central limit theorems for the Fréchet mean, further regularity conditions, and all technical proofs are provided in the supplementary material.

2 Preliminaries

2.1 Basic Settings

To facilitate our presentation throughout this article, we introduce the following notations and definitions. Let \mathcal{M} denote a d -dimensional Riemannian manifold equipped with a Riemannian metric g , which induces a geodesic distance function $\rho : \mathcal{M} \times \mathcal{M} \rightarrow \mathbb{R}$.¹ We denote by $\exp_p : T_p\mathcal{M} \rightarrow \mathcal{M}$ the exponential map at a point $p \in \mathcal{M}$, which sends a tangent vector $\mathbf{v} \in T_p\mathcal{M}$ to the point reached at unit time by the geodesic starting from p with initial velocity \mathbf{v} . While \exp_p is a local diffeomorphism near the origin, it is not globally injective; hence, multiple geodesics may connect two points $p, q \in \mathcal{M}$. The cut locus of p , denoted by $C(p)$, is the set of points where \exp_p ceases to be minimizing or injective. Equivalently, $C(p)$ consists of points connected to p by more than one minimizing geodesic. On $\mathcal{M} \setminus C(p)$, the exponential map remains a smooth diffeomorphism, and its inverse is well defined. We denote this inverse by \log_p , following standard convention. Furthermore, we assume that \mathcal{M} is geodesically complete, which ensures that (\mathcal{M}, ρ) forms a complete metric space. The remaining notations are summarized in Table 6 in Appendix A.

2.2 Fréchet Mean on Riemannian Manifold

Definition 1. Let \mathbb{P} be a probability measure on \mathcal{M} . The population Fréchet function is defined by $F(p) = \int_{\mathcal{M}} \rho^2(p, x) \mathbb{P}(dx)$, the population Fréchet mean set of \mathbb{P} is the set of minimizers of F and the corresponding minimum value is population Fréchet variance. Similarly, given an i.i.d. sample X_1, \dots, X_n , the sample Fréchet mean set

¹We assume that g is C^∞ -smooth.

is the set of minimizers of the sample Fréchet function $\hat{F}_n(p) = 1/n \sum_{i=1}^n \rho^2(p, X_i)$, and the corresponding minimum value is sample Fréchet variance.

Unlike its Euclidean counterpart, the existence and uniqueness of the Fréchet mean require careful consideration on a general manifold. For simplicity, we assume that the support of \mathbb{P} lies within a convex geodesic ball, which is sufficient to ensure both existence and uniqueness. This condition is stated formally in Assumption 1.

Assumption 1. *The support of the probability measure \mathbb{P} is contained in a closed geodesic ball $B(m_0, r)$ with some center m_0 and radius $r < \pi/(4\sqrt{\kappa})$, where κ is an upper bound on the sectional curvatures of \mathcal{M} . If $\kappa \leq 0$, then any $r < \infty$ suffices.*

We refer the reader to [Bhattacharya and Patrangenaru \[2003\]](#), [Bhattacharya and Bhattacharya \[2012\]](#) for a more comprehensive review on this topic. Under Assumption 1, the population and sample Fréchet mean exist and are unique, we denote them as η and $\hat{\eta}_n$, and the population and sample Fréchet variance as V and \hat{V}_n , respectively.

2.3 Differential Privacy

Definition 2. A mechanism \mathbb{M} is said to satisfy (ϵ, δ) -differential privacy if, for all measurable subsets S of its output space and for all neighbouring datasets D and D' differing in one individual, $\mathbb{P}[\mathbb{M}(D) \in S] \leq e^\epsilon \mathbb{P}[\mathbb{M}(D') \in S] + \delta$.

The parameters ϵ and δ jointly characterize the privacy loss, with smaller values indicating stronger protection. Since the (ϵ, δ) -DP definition is probabilistic, it is well defined on any probability space, including Riemannian manifolds equipped with the Borel σ -algebra. However, (ϵ, δ) -DP can be difficult to interpret or compose in high-dimensional settings. To address this issue, Gaussian Differential Privacy (GDP; [Dong et al., 2022](#)) characterizes privacy through the trade-off between type I

and type II errors in a binary hypothesis test distinguishing neighbouring datasets, quantified by a single privacy parameter μ .

Definition 3. A mechanism \mathbb{M} is said to satisfy μ -GDP if, for all neighbouring datasets D, D' , the corresponding output distributions $\mathbb{M}(D)$ and $\mathbb{M}(D')$ exhibit a Gaussian trade-off curve with privacy parameter μ .

Building on this framework, [Jiang et al. \[2023\]](#) extend Gaussian differential privacy (GDP) to Riemannian manifolds, formulating their approach around a key feature of GDP: its analytic equivalence to (ϵ, δ) -differential privacy. For any $\mu > 0$, a μ -GDP mechanism satisfies $(\epsilon, \delta_\mu(\epsilon))$ -DP for all $\epsilon \geq 0$, for $\delta_\mu(\epsilon) := \Phi(-\epsilon/\mu + \mu/2) - e^\epsilon \Phi(-\epsilon/\mu - \mu/2)$, where Φ denotes the cumulative distribution function of the standard normal distribution. This leads to the definition of GDP on Riemannian manifolds as follows.

Definition 4. A \mathcal{M} -valued data-releasing mechanism \mathbb{M} is said to be μ -GDP if it is $(\epsilon, \delta_\mu(\epsilon))$ -DP for all $\epsilon \geq 0$.

This formulation exploits the analytic equivalence between GDP and (ϵ, δ) -DP to give a concrete definition that avoids the technical complications of hypothesis-based formulations on manifolds. In particular, the mapping $\delta_\mu(\epsilon)$ provides a tractable way to express the privacy parameter μ , which quantifies the Gaussian trade-off between neighboring datasets as in the Euclidean case.

In the manifold setting, the privacy guarantee depends on the sensitivity of the released statistic with respect to the Riemannian metric. Formally, for a data-dependent mapping or a query, $f : \mathcal{D} \rightarrow \mathcal{M}$, its global sensitivity is defined as $\Delta := \sup_{D \simeq D'} \rho(f(D), f(D'))$.

The quantity Δ measures the maximal perturbation of the output induced by

replacing a single data point, capturing both the geometry of the manifold and the stability of the statistic. As in the Euclidean setting, the GDP privacy parameter μ is determined jointly by this sensitivity and the dispersion of the noise distribution. Consequently, achieving high utility requires careful calibration of the privacy budget μ against the noise dispersion parameter when enforcing differential privacy on manifolds.

3 Theoretical Results

In this section, we extend the GDP mechanism to the setting of Riemannian manifolds and establish the corresponding theoretical framework for statistical inference based on privatized Fréchet mean and variance. Specifically, we consider two categories of differential privacy mechanisms, respectively defined on homogeneous manifolds with positive curvature and on Hadamard manifolds.

3.1 DP Estimation of Fréchet Mean and Variance

For data $D = \{X_1, \dots, X_n\}$ i.i.d. from probability measure \mathbb{P} satisfying Assumption 1, we aim to construct differentially private Fréchet mean estimators $\hat{\eta}_n^{\text{dp}}$ by injecting \mathcal{M} -valued random noise to the sample Fréchet mean $\hat{\eta}_n$.

The manifold-valued noises ensure that the perturbed estimator remains on the manifold, unlike methods that embed $\hat{\eta}_n$ into an ambient Euclidean space and inject Euclidean noise. Achieving differential privacy requires a careful design of the noise injection, which motivates the construction of suitable privacy mechanisms.

Remark 1. *Note that under Assumption 1, the sensitivity of the sample Fréchet mean*

is, for κ an upper bound on the sectional curvatures of \mathcal{M} ,

$$\Delta_\eta = 2\lambda(r, \kappa)r/n, \text{ where } \lambda(r, \kappa) = \begin{cases} r^{-1}\kappa^{-1/2} \tan(\sqrt{\kappa}2r) - 1, & \kappa > 0; \\ 1, & \kappa \leq 0. \end{cases} \quad (1)$$

See [Reimherr et al. \[2021\]](#) for detailed derivations.

We introduce two privacy mechanisms, each tailored to a particular class of manifolds. The first, referred to as the Riemannian Gaussian (RG) mechanism, achieves GDP by injecting Riemannian Gaussian noise $\mathcal{N}^{\text{RG}}(\eta, \sigma)$, whose probability density function $p_{\eta, \sigma}(y)$ with respect to the Riemannian volume measure ν is

$$p_{\eta, \sigma}(y) := \frac{1}{Z(\eta, \sigma)} \exp\left\{-\frac{1}{2\sigma^2}\rho^2(y, \eta)\right\},$$

where η denotes the location parameter (the center), σ is the scale parameter governing the strength of privacy protection, and $Z(\eta, \sigma)$ is the normalizing constant.

In contrast to the RG mechanism, which operates directly on the manifold, the second mechanism, referred to as the Exponential-Wrapped Gaussian (EWG) mechanism, leverages the tangent-space structure. It achieves privacy by perturbing $\hat{\eta}_n$ with EWG noise $\mathcal{N}^{\text{EWG}}(p_0, \eta, \sigma)$, obtained by pushing forward the tangent-space Gaussian distribution $\mathcal{N}(\log_{p_0} \eta, \sigma^2 \mathbf{I}_d)$ on $T_{p_0}\mathcal{M}$ through the exponential map \exp_{p_0} .² Since this distribution is defined as the push-forward of a Gaussian law under \exp_{p_0} , it requires \exp_{p_0} to be injective on $T_{p_0}\mathcal{M}$. This condition naturally holds on Hadamard manifolds, where each tangent space is diffeomorphic to the manifold, ensuring the global injectivity of the exponential map.

In our implementation, for both the RG and EWG mechanisms, we set the center to $\hat{\eta}_n$. For the EWG mechanism we set the footpoint $p_0 = m_0$, where m_0 is defined

²For EWG distribution, we refer to the parameter p_0, η, σ as the footpoint, the center, and the scale parameter, respectively.

Algorithm 1 DP Fréchet Mean Estimation

Input: Sample Fréchet mean $\hat{\eta}_n$, data radius r , privacy budget μ , footpoint m_0 ;

Output: DP Fréchet mean estimate $\hat{\eta}_n^{\text{dp}}$;

- 1: **Let** $\sigma_{n,\eta} = \Delta_\eta / \mu$ with Δ_η given in (1).
 - 2: **if** \mathcal{M} is a homogeneous manifold of positive curvature **then**
 - 3: **Sample** $\hat{\eta}_n^{\text{dp}} \sim \mathcal{N}^{\text{RG}}(\hat{\eta}_n, \sigma_{n,\eta})$. ▷ RG mechanism
 - 4: **else if** \mathcal{M} is a Hadamard manifold **then**
 - 5: **Sample** $\hat{\eta}_n^{\text{dp}} \sim \mathcal{N}^{\text{EWG}}(m_0, \hat{\eta}_n, \sigma_{n,\eta})$. ▷ EWG mechanism
 - 6: **end if**
 - 7: **Return:** $\hat{\eta}_n^{\text{dp}}$.
-

in Assumption 1. For both mechanisms, the scale parameter σ controls the trade-off between privacy and accuracy.

Therefore, for these two representative classes of manifolds, we obtain the DP Fréchet mean estimator using the corresponding privacy mechanisms, as summarized in Algorithm 1.

Remark 2. *The footpoint p_0 used in the EWG mechanism can be any point within $B(m_0, r)$. However, the utility of the DP Fréchet mean estimator will be impacted by the location of p_0 and the curvature of the manifold. Ideally, one would use existing prior knowledge (if it exists) to select a footpoint near the sample Fréchet mean.*

A central challenge in designing privacy mechanisms lies in determining the quantitative relationship between σ and μ . In the original RG mechanism of Jiang et al. [2023], this relationship is defined implicitly through an infinite collection of inequalities, which makes direct implementation difficult. To address this issue, Jiang et al. [2023] employed an MCMC-based calibration procedure for μ ; however, this

approach applies only to manifolds of constant curvature—such as spheres, Euclidean spaces, and hyperbolic spaces—and incurs substantial computational cost.

We overcome both limitations by introducing an analytical calibration method for the privacy budget. Drawing on geometric comparison theory, we derive an explicit calibration formula for homogeneous manifolds of positive curvature. Likewise, for Hadamard manifolds, the proposed EWG mechanism admits a fully analytical calibration procedure. Fixing the privacy budget μ , we set $\sigma_{n,\eta} = \Delta_\eta/\mu$ for both mechanisms, rendering the overall implementation far more practical and computationally efficient. In a later section, we provide empirical comparisons showing that our derived lower bound for $\sigma_{n,\eta}$ is extremely tight. The privacy guarantee for Algorithm 1 is established by the following theorem.

Theorem 1 (Privacy Guarantee). *Under Assumption 1, the DP Fréchet mean estimator $\hat{\eta}_n^{\text{dp}}$, under both the RG and EWG mechanism in Algorithm 1, is μ -GDP.*

Next, we follow the same approach by injecting noise into the sample Fréchet variance \hat{V}_n . Since $\hat{V}_n \in \mathbb{R}$, Euclidean-valued noise is sufficient, and thus a traditional differential privacy (DP) mechanism can be applied. In particular, we employ the Gaussian mechanism to achieve GDP; that is, we sample

$$\hat{V}_n^{\text{DP}} \sim \mathcal{N}(\hat{F}_n(\hat{\eta}_n^{\text{dp}}), \sigma_{n,V}^2), \quad \hat{F}_n(p) = \frac{1}{n} \sum_{i=1}^n \rho^2(p, X_i),$$

where $\sigma_{n,V} = \Delta_{V_n}/\mu$ and $\Delta_{V_n} := \sup_{D \simeq D'} |\hat{F}_n(\hat{\eta}_n^{\text{dp}}) - \hat{F}'_n(\hat{\eta}_n^{\text{dp}})|$.³ We then obtain the following result for the privacy guarantee of our DP Fréchet variance estimator. The overall procedure is summarized in Algorithm 2, and its corresponding privacy guarantee is established in Theorem 2.

³Here $\hat{F}'_n(\cdot)$ denotes the sample Fréchet function w.r.t the neighboring dataset D' .

Algorithm 2 DP Fréchet Variance Estimation

Input: Data X_1, \dots, X_n , data radius r , DP Fréchet mean $\hat{\eta}_n^{\text{dp}}$, privacy budget μ ;

Output: DP Fréchet variance estimate \hat{V}_n^{dp} ;

- 1: **Compute** $\Delta_{V_n} = 4r^2/n$.
 - 2: **Compute** $\hat{F}_n(\hat{\eta}_n^{\text{dp}}) = 1/n \sum_{i=1}^n \rho^2(\hat{\eta}_n^{\text{dp}}, X_i)$.
 - 3: **Sample** $\hat{V}_n^{\text{dp}} \sim \mathcal{N}(\hat{F}_n(\hat{\eta}_n^{\text{dp}}), \sigma_{n,V}^2)$ with $\sigma_{n,V} = \Delta_{V_n}/\mu$.
 - 4: **Return:** \hat{V}_n^{dp} .
-

Theorem 2 (Privacy Guarantee for DP Fréchet Variance). *Under Assumption 1, given the DP Fréchet mean estimate $\hat{\eta}_n^{\text{dp}}$, the DP Fréchet variance estimator \hat{V}_n^{dp} in Algorithm 2 is μ -GDP with $\Delta_{V_n} = 4r^2/n$.*

3.2 Consistency and asymptotic normality

First, we start with the consistency of the DP Fréchet mean and variance estimators.

Theorem 3 (Consistency for DP Fréchet Mean). *Under Assumption 1, the DP Fréchet mean estimator $\hat{\eta}_n^{\text{dp}}$ in Algorithm 1 is a consistent estimator of η . Furthermore, we have $\rho(\hat{\eta}_n^{\text{dp}}, \eta) = \mathcal{O}_{\mathbb{P}}(n^{-1/2})$.*

This result is grounded in the observation that the global sensitivity of the sample Fréchet mean decays at the rate $\mathcal{O}(n^{-1})$, implying that the scale parameter of the differential privacy noise diminishes accordingly as the sample size n increases. This asymptotic vanishing of sensitivity forces the $\hat{\eta}_n^{\text{dp}}$ shrink into a local coordinate of η . In particular, the intrinsic geometry of the manifold can be locally approximated by the geometry of the tangent space at η .

Next, we derive the central limit results for the DP Fréchet mean estimator $\hat{\eta}_n^{\text{dp}}$.

We begin by defining the distance function with respect to the local coordinate chart (U, ϕ) centered at η to be $\rho_\phi(u, v) := \rho(\phi^{-1}(u), \phi^{-1}(v))$, for $u, v \in \phi(U)$. Denote

$$\Psi(u; \theta) = \text{grad}_\theta (\rho_\phi)^2(u, \theta) = \left(\frac{\partial}{\partial \theta^r} (\rho_\phi)^2(u, \theta) \right)_{r=1}^d = (\Psi^r(u; \theta))_{r=1}^d,$$

we define

$$\mathbf{C} := \text{Cov}[\Psi(\phi(X); \phi(\eta))], \quad \mathbf{\Lambda} := \mathbb{E} \left[\partial_r \Psi^{r'}(\phi(X), \phi(\eta)) \right]_{r, r'}^d. \quad (2)$$

Assumption 2. $\mathbf{\Lambda}$ is nonsingular and the following integrability conditions are satisfied:

$$\mathbb{E} [\|\Psi(\phi(X); \phi(\eta))\|] < \infty, \quad \mathbb{E} \left[\left| \partial_r \Psi^{r'}(\phi(X), \phi(\eta)) \right| \right] < \infty \quad \text{for } r, r' = 1, \dots, d.$$

Now we are ready to establish the distributional results:

Theorem 4 (Asymptotic Normality for DP Fréchet Mean). *Let \mathcal{M} be a Hadamard manifold or homogeneous manifold of positive curvature. Under Assumptions 1 and 2, for the DP Fréchet mean $\hat{\eta}_n^{\text{dp}}$ in Algorithm 1, one has for $n \rightarrow \infty$*

$$\left(\frac{1}{n} \mathbf{\Lambda}^{-1} \mathbf{C} \mathbf{\Lambda}^{-1} + \sigma_{n, \eta}^2 \mathbf{I}_d \right)^{-1/2} (\phi(\hat{\eta}_n^{\text{dp}}) - \phi(\eta)) \rightsquigarrow \mathcal{N}(\mathbf{0}, \mathbf{I}_d) \quad (3)$$

where $\mathbf{\Lambda}, \mathbf{C}$ are defined in (2). If \mathcal{M} is homogeneous manifold of positive curvature, we take $\phi := \log_\eta(\cdot)$. If \mathcal{M} is a Hadamard manifold, we take $\phi := \log_{m_0}(\cdot)$, where m_0 is defined in Assumption 1.

Compared with the CLT in Euclidean spaces, the main difference arises from the expected Hessian matrix $\mathbf{\Lambda}$ of the squared distance function ρ^2 . This matrix can be viewed as a quantity that characterizes how the manifold deviates from Euclidean geometry; it reduces to the multiple of identity matrix when the manifold is Euclidean. For more details about BP-CLT, we refer to Section S.1.8 in the supplementary material.

As an immediate consequence of Theorem 4, we can construct an asymptotically confidence region for population Fréchet mean η based on $\hat{\eta}_n^{\text{dp}}$ as follows.

Corollary 1 (Asymptotic Confidence Region for Fréchet Mean). *Under the assumptions and setups of Theorem 4, a DP $(1 - \alpha)$ -confidence region for η is given by*

$$\left\{ v \in \mathcal{M} \mid (\phi(\hat{\eta}_n^{\text{dp}}) - \phi(v))^\top \mathbf{\Gamma}_n^{-1} (\phi(\hat{\eta}_n^{\text{dp}}) - \phi(v)) \leq \chi_{d,1-\alpha}^2 \right\}, \quad (4)$$

where $\mathbf{\Gamma}_n := \frac{1}{n} \mathbf{\Lambda}^{-1} \mathbf{C} \mathbf{\Lambda}^{-1} + \sigma_{n,\eta}^2 \mathbf{I}_d$ and $\chi_{d,1-\alpha}^2$ denotes the $(1 - \alpha)$ -th quantile of the χ_d^2 distribution. If \mathcal{M} is a homogeneous manifold of positive curvature, we take $\phi := \log_{\hat{\eta}_n^{\text{dp}}}(\cdot)$. If \mathcal{M} is a Hadamard manifold, we take $\phi := \log_{m_0}(\cdot)$.

The CLT for Fréchet means on Riemannian manifolds can behave subtly, as shown by [Eltzner and Huckemann \[2019\]](#), who identified smeariness on spheres when Assumption 1 fails. In this regime, the convergence slows to below the usual $n^{-1/2}$ rate. Nevertheless, in our DP framework, the convergence rate remains governed by the non-DP CLT rate, and an analogous result extends to the smeary-CLT setting (see Section S.3 of the supplementary material).

Next, we present the asymptotic normality for \hat{V}_n^{dp} with additional regularity conditions stated in Section S.1.10 of the supplementary material.

Theorem 5 (Asymptotic Normality for DP Fréchet Variance). *Under Assumptions 1 and S.1.2, for DP Fréchet variance estimator in Algorithm 2, one has,*

$$\left(\frac{1}{n} \sigma_F^2 + \sigma_{n,V}^2 \right)^{-1/2} \left(\hat{V}_n^{\text{dp}} - V \right) \rightsquigarrow \mathcal{N}(0, 1)$$

where $\sigma_F^2 := \text{var}(\rho^2(X, \eta))$.

Analogous to the Fréchet mean setting, we can construct an asymptotic confidence region for the Fréchet variance V .

Corollary 2 (Asymptotic Confidence Interval for DP Fréchet Variance). *Under Assumptions 1 and S.1.2, a DP $(1 - \alpha)$ -confidence interval for V is given by*

$$\left(\hat{V}_n^{\text{dp}} - z_{1-\alpha/2} \sqrt{\frac{1}{n} \sigma_F^2 + \sigma_{n,V}^2}, \hat{V}_n^{\text{dp}} + z_{1-\alpha/2} \sqrt{\frac{1}{n} \sigma_F^2 + \sigma_{n,V}^2} \right) \quad (5)$$

where $z_{1-\alpha/2}$ denotes the $(1 - \alpha/2)$ -th quantile of the standard normal distribution.

4 Implementation

In (4) and (5), Γ_n and σ_F^2 are unknown and thus must be estimated privately. We will discuss the details of the private estimation in this section.

4.1 Estimating Limiting Variance for Fréchet Mean

Recall that the limiting covariance matrix for the Fréchet mean in Theorem 4 is of the form

$$\frac{1}{n} \Lambda^{-1} \mathbf{C} \Lambda^{-1} + \sigma_{n,\eta}^2 \mathbf{I}_d,$$

where the matrices Λ and \mathbf{C} are defined in (2). To construct DP estimators for Λ and \mathbf{C} , we begin with their sample versions,

$$\hat{\Lambda}_n = \frac{1}{n} \sum_{i=1}^n \left[\partial_r \Psi^{r'}(\phi(X_i), \phi(\hat{\eta}_n)) \right]_{r,r'=1}^d, \quad \hat{\mathbf{C}}_n = \widehat{\text{Cov}}[\Psi(\phi(X); \phi(\eta))],$$

where $\widehat{\text{Cov}}$ denotes the sample covariance. In particular, we note that

$$\Psi(\phi(X); \phi(\eta)) = -2[D_{\phi(\eta)} \phi^{-1}]^\dagger(\log_\eta(X)),$$

where \dagger denotes the adjoint operator. It follows that, $\hat{\mathbf{C}}_n = 4L_{\phi,\eta}^\dagger \widehat{\text{Cov}}(\log_\eta(X)) L_{\phi,\eta}$,

where $L_{\phi,\eta} := D_{\phi(\eta)} \phi^{-1}$. Note that since we take $\phi := \log_\eta(\cdot)$ in the case of RG mechanism for Homogeneous manifolds of positive curvature, we have $L_{\phi,\eta} = \mathbf{I}$. On

the other hand, we take $\phi := \log_{m_0}(\cdot)$ in the case of EWG mechanism for Hadamard manifolds, we have $L_{\phi, \eta} = D_{\log_{m_0}(\eta)} \exp_{m_0}$. In both cases, we replace the η in $\hat{\Lambda}_n$ and \hat{C}_n with the DP estimator $\hat{\eta}_n^{\text{dp}}$:

$$\tilde{\Lambda}_n = \frac{1}{n} \sum_{i=1}^n \left[\partial_r \Psi^{r'} \left(\phi(X_i), \phi(\hat{\eta}_n^{\text{dp}}) \right) \right]_{r, r'}^d, \quad \tilde{C}_n = 4L_{\phi, \hat{\eta}_n^{\text{dp}}}^\dagger \widehat{\text{Cov}}(\log_{\hat{\eta}_n^{\text{dp}}}(X)) L_{\phi, \hat{\eta}_n^{\text{dp}}}. \quad (6)$$

Because individual observations X_i enter both $\tilde{\Lambda}_n$ and $\widehat{\text{Cov}}(\log_{\hat{\eta}_n^{\text{dp}}}(X))$, these statistics leak private information; consequently, additional privacy protection is required. First, we note that $\tilde{\Lambda}_n$ and $\widehat{\text{Cov}}(\log_{\hat{\eta}_n^{\text{dp}}}(X))$ are SPDMS, and the sum of two SPDMS is again an SPDMS. Thus, we consider the half-vectorization of $\tilde{\Lambda}_n$ and $\widehat{\text{Cov}}(\log_{\hat{\eta}_n^{\text{dp}}}(X))$ via the `vecd` operator (see [Schwartzman \[2016\]](#) for more details). It follows that we can obtain DP versions of the sample estimators by perturbing their half-vectorizations:

$$\hat{\Lambda}_n^{\text{dp}} := \text{vecd}^{-1} \left[\text{vecd}(\tilde{\Lambda}_n) + \mathcal{N}(\mathbf{0}, \sigma_\Lambda^2 \mathbf{I}_{d(d+1)/2}) \right], \quad (7)$$

$$\hat{C}_n^{\text{dp}} := 4L_{\phi, \hat{\eta}_n^{\text{dp}}}^\dagger \text{vecd}^{-1} \left[\text{vecd}(\widehat{\text{Cov}}(\log_{\hat{\eta}_n^{\text{dp}}}(X))) + \mathcal{N}(\mathbf{0}, \sigma_C^2 \mathbf{I}_{d(d+1)/2}) \right] L_{\phi, \hat{\eta}_n^{\text{dp}}}, \quad (8)$$

where $\sigma_\Lambda = \Delta_\Lambda / \mu$, $\sigma_C = \Delta_C / \mu$, Δ_Λ and Δ_C denote the ℓ_2 sensitivities of $\text{vecd}(\tilde{\Lambda})$, and $\text{vecd}(\widehat{\text{Cov}}(\log_{\hat{\eta}_n^{\text{dp}}}(X)))$, respectively.

Lastly, we need to evaluate the sensitivities Δ_Λ and Δ_C . To bound these quantities, we impose the following assumption.

Assumption 3. *Given $\hat{\eta}_n^{\text{dp}}$, $\|\log_{\hat{\eta}_n^{\text{dp}}}(X_i)\|_F \leq R$ for all $1 \leq i \leq n$.*

Note that if Assumption 1 holds, then Assumption 3 is satisfied with $R = 2r$. Alternatively, one may set $R = r$ by truncating $\phi(X_i)$ so that $\|\log_{\hat{\eta}_n^{\text{dp}}}(X_i)\| \leq r$.

To bound the sensitivity Δ_Λ , we require the following condition on the Hessian of the squared distance function.

Assumption 4. Given $\hat{\eta}_n^{\text{dp}}$, denote $H_i := \left[\partial_r \Psi^{r'}(\phi(X), \phi(\hat{\eta}_n)) \right]_{r,r'}^d$, we have $\|H_i\|_F \leq B_H$ for $1 \leq i \leq n$.

Theorem 6. Under Assumptions 3 and 4, we have $\Delta_C \leq 6R^2/n$ and $\Delta_\Lambda \leq 2B_H/n$.

Furthermore, the DP limiting covariance estimator,

$$\hat{\mathbf{\Gamma}}_n^{\text{dp}} := \frac{1}{n} \left(\hat{\mathbf{\Lambda}}_n^{\text{dp}} \right)^{-1} \hat{\mathbf{C}}_n^{\text{dp}} \left(\hat{\mathbf{\Lambda}}_n^{\text{dp}} \right)^{-1} + \sigma_{n,\eta}^2 \mathbf{I}_d,$$

together with the DP Fréchet mean estimate $\hat{\eta}_n^{\text{dp}}$ is $\sqrt{3}\mu$ -GDP, where $\hat{\mathbf{\Lambda}}_n^{\text{dp}}$ and $\hat{\mathbf{C}}_n^{\text{dp}}$ are defined in (7) and (8), respectively. Lastly, $\hat{\mathbf{\Lambda}}_n^{\text{dp}}$ and $\hat{\mathbf{C}}_n^{\text{dp}}$ are consistent estimators of $\mathbf{\Lambda}$ and \mathbf{C} , respectively.

To estimate the unknown limiting variance of the DP Fréchet variance estimator, it is sufficient to estimate σ_F^2 privately. Denote the sample estimator of σ_F^2 by

$$\hat{\sigma}_F^2 := \frac{1}{n} \sum_{i=1}^n \rho^4(X_i, \hat{\eta}_n) - \left(\frac{1}{n} \sum_{i=1}^n \rho^2(X_i, \hat{\eta}_n) \right)^2 = \frac{1}{n} \sum_{i=1}^n \rho^4(X_i, \hat{\eta}_n) - \left(\hat{V}_n \right)^2$$

Analogous to \hat{V}_n^{dp} , we apply the (Euclidean) Gaussian mechanism for GDP to obtain a DP estimator of σ_F^2 . Specifically, denote

$$\begin{aligned} \tilde{\sigma}_F^2 &:= \frac{1}{n} \sum_{i=1}^n \rho^4(X_i, \hat{\eta}_n^{\text{dp}}) - \left(\hat{V}_n^{\text{dp}} \right)^2, \\ \Delta_\sigma &:= \sup_{D \simeq D'} \left| \frac{1}{n} \sum_{i=1}^n \rho^4(X_i, \hat{\eta}_n^{\text{dp}}) - \frac{1}{n} \sum_{i=1}^n \rho^4(X'_i, \hat{\eta}_n^{\text{dp}}) \right|, \end{aligned}$$

we generate the DP estimator for σ_F^2 as $\hat{\sigma}_F^{2,\text{dp}} := \tilde{\sigma}_F^2 + \mathcal{N}(0, \Delta_\sigma^2/\mu^2)$. This yields a privatized estimator for the limiting variance, as formalized in the following result.

Theorem 7 (Privacy and Consistency Guarantee for DP σ_F^2 Estimator). *Under Assumption 1, given the DP estimates $\hat{\eta}_n^{\text{dp}}, \hat{V}_n^{\text{dp}}$, the DP limiting variance estimator $\hat{\sigma}_F^{2,\text{dp}} \sim \mathcal{N}(\tilde{\sigma}_F^2, \sigma^2)$ with $\sigma = \Delta_\sigma/\mu$ is μ -GDP where $\Delta_\sigma = 16r^4/n$. Furthermore, $\hat{\sigma}_F^{2,\text{dp}}$ is a consistent estimator of σ_F^2 .*

5 Numerical experiments

In this section, we evaluate our DP estimators and confidence regions on simulated data from the unit sphere and the SPD space.

For the unit sphere S^d , a canonical example of a homogeneous manifold with positive curvature and therefore an ideal testbed for our methodology, we set $d = 2$ and generate datasets $D = (X_1, \dots, X_n)$ by first sampling uniformly from the geodesic ball $B(\eta, \pi/8) \subset S^2$, where the centre η is redrawn at random for each replication. For the space of symmetric positive definite matrices S_m^+ , with $m = 2$, we generate data $D = \{X_1, \dots, X_n\}$ by first sample uniformly from the geodesic ball $B(\mathbf{0}, 1.5)$ on the tangent space $T_{\mathbf{I}_m} S_m^+$ and then map to S_m^+ via $\exp_{T_{\mathbf{I}_m}}(\cdot)$. We endow S_m^+ with the Fisher–Rao affine-invariant metric, under which S_m^+ forms a Hadamard manifold with strictly negative sectional curvature. We refer readers to Section S.1.7 of the supplementary material for further details on this metric.

The sample size is fixed at $n = 600$ for both the Fréchet mean and Fréchet variance, while the privacy budget varies over $\mu \in \{0.1, 0.2, \dots, 2.5\}$. The number of Monte Carlo replications is 1000.

For each privacy level, we compute the sample Fréchet mean $\hat{\eta}_n$ from D using a gradient descent algorithm, together with the corresponding sample Fréchet variance \hat{V}_n . We then construct the differentially private Fréchet mean estimator $\hat{\eta}_n^{\text{dp}}$ and variance estimator \hat{V}_n^{dp} according to Algorithms 1 and 2. For each Monte Carlo replication, we record $\rho(\hat{\eta}_n, \eta)$, $\rho(\hat{\eta}_n^{\text{dp}}, \eta)$, $|\hat{V}_n - V|$, and $|\hat{V}_n^{\text{dp}} - V|$. We summarize these errors by their Monte Carlo means, denoted MD (mean distance), and report them in Tables 1 and 2. As shown in both tables, the gap between the MDs of the DP and non-DP estimators shrinks as the privacy budget increases.

It is worth noting that the values μ^* in Table 1 are obtained using an MCMC-based procedure that computes the exact (analytical) privacy budget corresponding to a given noise level $\sigma_{n,\eta}$ and sensitivity Δ_η . For a target privacy budget μ , our implementation instead employs the lower bound in Algorithm 1 to obtain a fast approximation to $\sigma_{n,\eta}$; we then compute the associated exact privacy budget μ^* as well. The results show that our lower bound is extremely close to the exact value while avoiding the substantial computational cost of the MCMC calibration, thereby making the DP inference framework more practical and efficient.

To construct confidence regions for the Fréchet mean, we estimate the two components of the limiting covariance, $\hat{\Lambda}_n$ and \hat{C}_n . The non-DP confidence region is obtained by substituting Λ and C in Corollary 1 with their sample estimates $\hat{\Lambda}_n$ and \hat{C}_n , and by setting $\sigma_{n,\eta} = 0$. To generate the DP confidence region, we use the differentially private estimators $\hat{\Lambda}_n^{\text{dp}}$ and \hat{C}_n^{dp} defined in (7) and (8), plug them into Corollary 1, and set $\sigma_{n,\eta} = \Delta_\eta/(\mu/\sqrt{3})$.

Similarly, for Fréchet variance, we split the privacy budget by allocating $\mu/\sqrt{3}$ to $\hat{\eta}_n^{\text{dp}}$, \hat{V}_n^{dp} and to $\hat{\sigma}_F^{2,\text{dp}}$, following the corresponding theoretical guarantee. We report the finite-sample coverage of the DP confidence regions at significance level $\alpha = 0.05$ in Tables 1–4. Empirically, the coverage rates of the DP asymptotic confidence regions for both the Fréchet mean and variance remain close to the nominal level across most settings. In a few cases involving the Fréchet variance, the coverage rate is slightly below the nominal level, which may be attributed to the fact that the estimator $\hat{\sigma}_F^{2,\text{dp}}$ can occasionally underestimate $\hat{\sigma}_F^2$.

For visualization of confidence region coverage, we pull back both the DP and non-DP confidence regions to their respective tangent spaces for direct comparison.

In the non-DP setting, the constructed confidence region is pulled back to the tangent space $T_{\hat{\eta}_n} S^2$ via $\log_{\hat{\eta}_n}$ and is represented by red ellipses in Figure 3. The population Fréchet mean η is likewise mapped to $T_{\hat{\eta}_n} S^2$ as $\log_{\hat{\eta}_n} \eta$, shown as triangular red points.

In the DP setting, the DP confidence region and the population Fréchet mean are pulled back to $T_{\hat{\eta}_n^{\text{dp}}} S^2$ via $\log_{\hat{\eta}_n^{\text{dp}}}$, and are visualized as blue ellipses and circular blue points, respectively. As illustrated in Figure 3, the DP confidence regions progressively approach their non-DP counterparts as the privacy budget μ increases.

Table 1: Fréchet mean results on sphere. Top row: MD of DP sample Fréchet mean. Bottom row: Coverages of DP confidence regions for Fréchet mean.

μ	0.1	0.2	0.3	0.5	0.7	1	1.5	2	2.5	non-DP
μ^*	0.099	0.199	0.300	0.500	0.700	0.999	1.500	2.000	2.500	–
MD (10^{-4})	183	126	116	106	106	107	105	105	103	103
coverage	0.941	0.953	0.945	0.96	0.954	0.939	0.941	0.954	0.96	0.954

Table 2: Fréchet variance results on sphere. Top row: MD of DP sample Fréchet variance. Bottom row: Coverages of DP confidence regions for Fréchet variance.

μ	0.1	0.2	0.3	0.5	0.7	1	1.5	2	2.5	non-DP
MD (10^{-5})	137	73.9	51.1	31.8	25.6	21.5	17.6	16.2	16.4	14.6
coverage	0.957	0.944	0.928	0.941	0.931	0.924	0.938	0.942	0.931	0.947

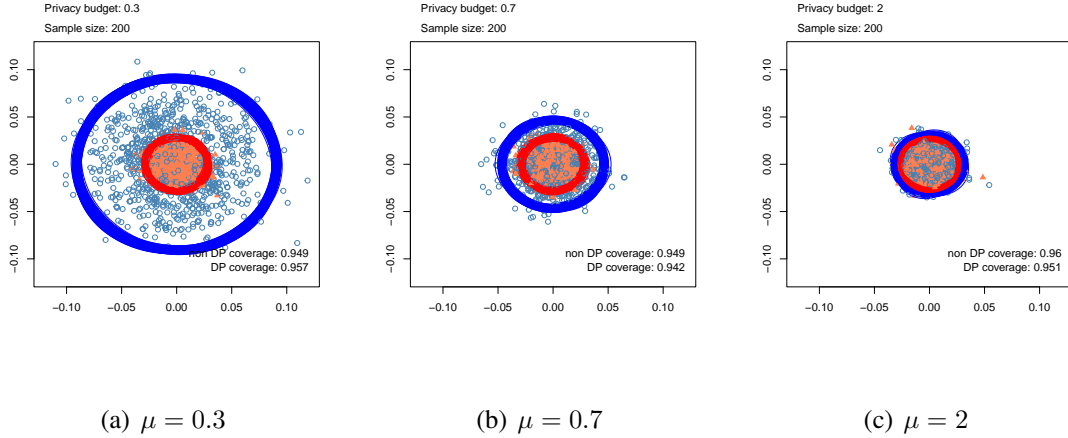


Figure 3: Visualization of the coverage of confidence regions. The blue ellipses and points indicate the DP confidence regions, while the red ellipses and points indicate the non-DP confidence regions.

Table 3: Fréchet mean results on SPDM space. Top row: MD of DP sample Fréchet mean. Bottom row: Coverages of DP confidence regions for Fréchet mean.

μ	0.1	0.2	0.3	0.5	0.7	1	1.5	2	2.5	non-DP
MD (10^{-3})	144	78.1	59.9	46.6	42.1	40.1	39.4	38.2	38	37.7
coverage	0.945	0.943	0.942	0.95	0.96	0.966	0.966	0.962	0.964	0.971

6 Applications to Real Datasets

6.1 Medical image data

The first dataset, OCTMNIST, is from the MedMNIST collection [Yang et al., 2021a,b], which contains 28×28 grayscale OCT images resized from 109,309 valid retinal OCT scans. After preprocessing, each image is mapped to a 5×5 SPD covariance descriptor in S_5^+ (see Section S.3 in the supplementary material).

The OCTMNIST dataset contains four classes, labeled 0–3. For each class, we construct DP and non-DP $(1 - \alpha)$ confidence regions for the Fréchet mean with

Table 4: Fréchet variance results on SPDM space. Top row: MD of DP sample Fréchet variance.

Bottom row: Coverages of DP confidence regions for Fréchet variance.

μ	0.1	0.2	0.3	0.5	0.7	1	1.5	2	2.5	non-DP
MD (10^{-4})	207	105	71.6	46.4	34.9	29.2	22.9	21.4	20.8	19.7
coverage	0.95	0.964	0.939	0.948	0.937	0.937	0.946	0.947	0.95	0.954

$\alpha = 0.05$. We summarize the estimated asymptotic covariance $\hat{\Gamma}_n^{\text{dp}}$ by its three largest eigenvalues and the explained proportion $(\lambda_1 + \lambda_2 + \lambda_3)/\text{tr}(\hat{\Gamma}_n^{\text{dp}})$, and report the effective radius $(\text{tr}(\hat{\Gamma}_n^{\text{dp}}))^{1/2}$, volume $(\det(\hat{\Gamma}_n^{\text{dp}}))^{1/2}$, and the distortion $d(\hat{\eta}_n, \hat{\eta}_n^{\text{dp}})$.

Table 5 reports the results for Class 0; results for the remaining classes are given in Section S.3 of the supplementary material.

For visualization, we project each confidence ellipsoid onto the first three coordinates of $T_{I_5}S_5^+$ and plot the resulting 3D slices (Figure 4). Moderate privacy ($\mu = 1, 2$) yields DP regions close to their non-DP counterparts, whereas strong privacy ($\mu = 0.1$) inflates the region and reduces the explained proportion, indicating that uncertainty spreads beyond the first three coordinates. Classes with tighter embeddings (e.g., Class 0 and Class 3) exhibit smaller regions, reflecting lower within-class variability under this SPD representation.

6.2 Sociology data

The second dataset is the sociology data of Fisher et al. [1987]. In a study of 48 individuals' attitudes toward 16 occupations, judgments were made according to four criteria: Earnings, Social Status, Reward, and Social Usefulness. This produced four samples of 48 multivariate observations. Using external analysis, each

Table 5: Results for Class 0 in the OCTMNIST dataset. See Section S.3 of the supplementary material for the results of other classes.

	λ_1	λ_2	λ_3	ratio	rad	vol	dist
0.1	0.029	0.008	0.005	0.714	0.242	$3.32_{(10^{-21})}$	0.139
1	0.026	0.005	0.002	0.928	0.190	$2.60_{(10^{-31})}$	0.014
2	0.026	0.005	0.002	0.935	0.189	$2.63_{(10^{-33})}$	0.007
non-DP	0.026	0.005	0.002	0.942	0.188	$1.96_{(10^{-39})}$	

observation was reduced to a unit (spherical) vector, yielding four samples of unit vectors corresponding to the four criteria.

For each criterion, we construct both non-DP and DP asymptotic confidence regions for the Fréchet mean. For the DP regions, we truncate the data to lie within the geodesic ball centered at the sample Fréchet mean with radius $\pi/8$, and display the resulting 95% confidence regions for privacy budgets $\mu = 1$ and $\mu = 2$ in Figure 5. Consistent with the behaviour observed in Section 5, the DP confidence regions contract towards their non-DP counterparts as the privacy budget increases. For ease of comparison across criteria, the results for Social Status and Reward are plotted together in the last column of Figure 5. In the original non-private analysis, the 95% regions for these two criteria overlap only slightly, indicating that the latent patterns of occupational evaluation are similar but not identical, nearby in direction, yet compatible with distinct underlying populations [Fisher et al., 1987, Chapter 7]. Under $\mu = 2$, the DP regions are very close to the non-DP ones, and the limited overlap again suggests related but genuinely different directional patterns. When μ is reduced to 1, the DP regions expand and overlap more, reflecting increased uncertainty under the stronger privacy constraint; nevertheless, each DP Fréchet mean still lies outside

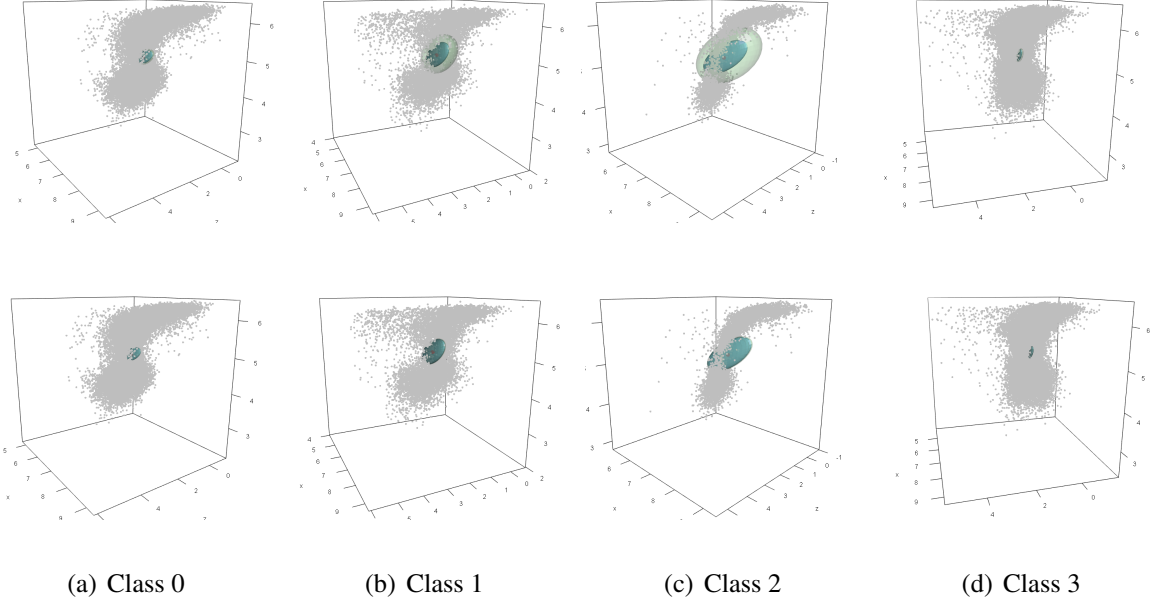


Figure 4: DP (green) and non-DP (blue) confidence regions projected to the tangent space at \mathbf{I}_5 using the first three coordinates. The top and bottom rows correspond to privacy budgets $\mu = 0.1$ and $\mu = 1$, respectively.

the other’s 95% DP region, so the central directions remain separated. In practical terms, if the two regions were to overlap almost completely, we would regard the latent occupational evaluation patterns as essentially the same; even under stronger privacy, however, they remain sufficiently distinct to support a meaningful directional difference between the two criteria.

7 Concluding remarks

This work addresses the gap at the intersection of geometry and privacy by developing principled, implementable differential privacy mechanisms and inference procedures for manifold-valued data, with a focus on Fréchet mean and variance on widely used spaces such as Hadamard manifolds or homogeneous manifolds with positive

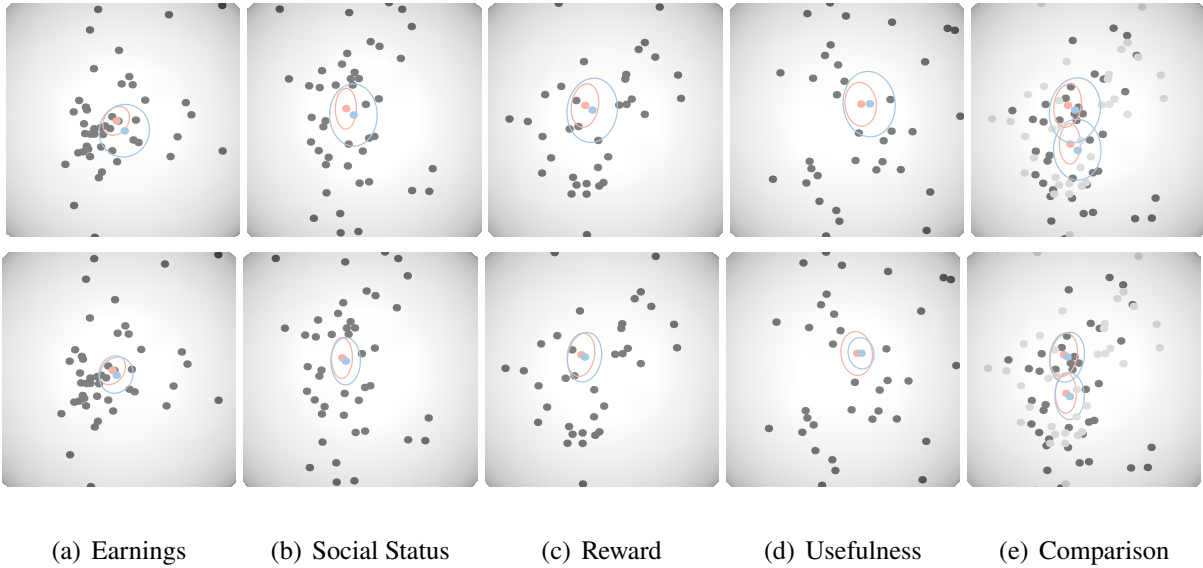


Figure 5: DP asymptotic confidence regions constructed on sociology data. The region outlined by the red ellipse indicates the non-DP confidence region, while the blue ellipse indicates the DP confidence region. The top and bottom rows correspond to privacy budgets of $\mu = 1, 2$, respectively.

curvature. By tying noise calibration to intrinsic geometric sensitivity, our framework preserves the spirit of Euclidean DP while respecting curvature and the lack of linear structure, and it delivers root- n consistency, CLTs, and smeary asymptotics that enable valid uncertainty quantification under privacy constraints. The resulting estimators are fully practical, avoiding bespoke MCMC or opaque budget inversions, and thus suitable for sensitive real world applications.

Despite these advances, our framework has limitations. Our methods are formulated under central DP with a trusted aggregator and thus do not provide local privacy against the curator. Extending DP inference to a local model on manifolds presents additional challenges, owing to the nonlinear geometry. Addressing these issues represents an interesting direction for future work.

A Notations

Table 6: Notations Table

Symbol	Description
\mathcal{M}	Riemannian manifold with dimension d
g	Riemannian metric (inner product on tangent spaces)
$\rho(p, q)$	Geodesic distance between points $p, q \in \mathcal{M}$
ν	Riemannian volume measure on \mathcal{M}
$\exp_p(\log_p)$	Riemannian exponential (logarithmic) map at point p
$\text{Exp}(\text{Log})$	Matrix exponential (logarithm)
$B(p, r)$	Geodesic ball centered at $p \in \mathcal{M}$ with radius r , $\{x \in \mathcal{M} \mid \rho(x, p) \leq r\}$
$\eta_{\mathbb{P}}$	Population Fréchet mean w.r.t. distribution \mathbb{P}
$\hat{\eta}_n, \hat{V}_n$ and \hat{F}_n	Sample Fréchet mean, variance and function
$\hat{\eta}_n^{\text{dp}}$	DP sample Fréchet mean
$\{X_i\}_{i=1}^n$	Confidential data sample from some unknown distribution \mathbb{P} on \mathcal{M}
σ	Rate parameter in Gaussian or Laplace mechanism
μ	Privacy budget for GDP
S_m^+	Space of $m \times m$ SPD matrices
ρ^{AI}	Affine-Invariant distance on S_m^+
S_m	Space of $m \times m$ symmetric matrices
vecd	Vectorization map from S_m to \mathbb{R}^d
Σ and $\hat{\Sigma}$	Asymptotic covariance matrix and its sample estimator
$D_x f$	Differential of map f at x
$\text{Hess}_x f$	Hessian of map f at x
$\text{Supp}(\mathbb{P})$	The support of a probability \mathbb{P}
$C(p)$	The cut locus of p

B Supplementary material

The supplementary material contains backgrounds of Riemannian manifolds, additional results for data applications and detailed proofs of the theoretical results.

References

- P. J. Basser, J. Mattiello, and D. LeBihan. Mr diffusion tensor spectroscopy and imaging. *Biophysical journal*, 66(1):259–267, 1994.
- G. Becigneul and O.-E. Ganea. Riemannian adaptive optimization methods. In *International Conference on Learning Representations*, 2019.
- S. Bhattacharjee, B. Li, and L. Xue. Nonlinear global fréchet regression for random objects via weak conditional expectation. *arXiv:2310.07817*, 2023.
- A. Bhattacharya and R. Bhattacharya. *Nonparametric Inference on Manifolds: With Applications to Shape Spaces*. IMS monograph. Cambridge University Press, 2012. ISBN 9781107019584.
- R. Bhattacharya and V. Patrangenaru. Large sample theory of intrinsic and extrinsic sample means on manifolds. *The Annals of Statistics*, 31(1):1 – 29, 2003.
- R. Bhattacharya and V. Patrangenaru. Large sample theory of intrinsic and extrinsic sample means on manifolds—II. *The Annals of Statistics*, 33(3):1225 – 1259, 2005.
- M. Blanchard and A. Q. Jaffe. Fréchet mean set estimation in the hausdorff metric, via relaxation. *Bernoulli*, 31(1):432–456, 2025.

- R. Chakraborty and B. C. Vemuri. Statistics on the stiefel manifold: Theory and applications. *The Annals of Statistics*, 47(1):415–438, 2019.
- J. Dong, A. Roth, and W. J. Su. Gaussian differential privacy. *Journal of the Royal Statistical Society: Series B (Statistical Methodology)*, 84(1):3–37, 2022.
- P. Dubey and H.-G. Müller. Fréchet analysis of variance for random objects. *Biometrika*, 106(4):803–821, 2019.
- P. Dubey and H.-G. Müller. Fréchet change-point detection. *The Annals of Statistics*, 48(6):3312–3335, 2020a.
- P. Dubey and H.-G. Müller. Functional models for time-varying random objects. *Journal of the Royal Statistical Society Series B: Statistical Methodology*, 82(2): 275–327, 2020b.
- P. Dubey, Y. Chen, and H.-G. Müller. Metric statistics: Exploration and inference for random objects with distance profiles. *The Annals of Statistics*, 52(2):757–792, 2024.
- C. Dwork, K. Kenthapadi, F. McSherry, I. Mironov, and M. Naor. Our data, ourselves: Privacy via distributed noise generation. In *Proceedings of the 24th Annual International Conference on The Theory and Applications of Cryptographic Techniques*, EUROCRYPT’06, page 486–503, Berlin, Heidelberg, 2006. Springer-Verlag.
- B. Eltzner and S. F. Huckemann. A smeary central limit theorem for manifolds with application to high-dimensional spheres. *The Annals of Statistics*, 47(6):3360 – 3381, 2019.

- S. N. Evans and A. Q. Jaffe. Limit theorems for fréchet mean sets. *Bernoulli*, 30(1): 419–447, 2024.
- N. I. Fisher, T. Lewis, and B. J. J. Embleton. *Statistical Analysis of Spherical Data*. Cambridge University Press, 1987.
- J. M. Jeon, B. U. Park, and I. Van Keilegom. Additive regression for non-euclidean responses and predictors. *The Annals of Statistics*, 49(5):2611–2641, 2021.
- Y. Jiang, X. Chang, Y. Liu, L. Ding, L. Kong, and B. Jiang. Gaussian differential privacy on riemannian manifolds. *Advances in Neural Information Processing Systems*, 36:14665–14684, 2023.
- M. Jordan, T. Lin, and E.-V. Vlatakis-Gkaragkounis. First-order algorithms for min-max optimization in geodesic metric spaces. In S. Koyejo, S. Mohamed, A. Agarwal, D. Belgrave, K. Cho, and A. Oh, editors, *Advances in Neural Information Processing Systems*, volume 35, pages 6557–6574. Curran Associates, Inc., 2022.
- H. Kasai, P. Jawanpuria, and B. Mishra. Riemannian adaptive stochastic gradient algorithms on matrix manifolds. In *International conference on machine learning*, pages 3262–3271. PMLR, 2019.
- J. Lee and S. Jung. Huber means on riemannian manifolds. *Journal of the Royal Statistical Society Series B: Statistical Methodology*, page qkaf054, 08 2025. ISSN 1369-7412.
- L. Lin and Z. Chen. A type of nonlinear fréchet regressions. *arXiv:2403.17481*, 2024.

- Z. Lin and F. Yao. Functional regression on the manifold with contamination. *Biometrika*, 108(1):167–181, 2021.
- Y. Liu, Q. Hu, L. Ding, and L. Kong. Online local differential private quantile inference via self-normalization. In *International Conference on Machine Learning*, pages 21698–21714. PMLR, 2023.
- Y. Liu, Q. Hu, and L. Kong. Tuning-free estimation and inference of cumulative distribution function under local differential privacy. In *Forty-first International Conference on Machine Learning*, 2024.
- K. V. Mardia and P. E. Jupp. *Directional statistics*. John Wiley & Sons, 2000.
- A. McCormack and P. Hoff. Equivariant estimation of fréchet means. *Biometrika*, 110(4):1055–1076, 2023.
- X. Pennec, S. Sommer, and T. Fletcher. *Riemannian geometric statistics in medical image analysis*. Academic Press, 2019.
- A. Petersen and H.-G. Müller. Fréchet regression for random objects with euclidean predictors. *The Annals of Statistics*, 47(2):691–719, 2019.
- M. Reimherr, K. Bharath, and C. Soto. Differential privacy over riemannian manifolds. In M. Ranzato, A. Beygelzimer, Y. Dauphin, P. Liang, and J. W. Vaughan, editors, *Advances in Neural Information Processing Systems*, volume 34, pages 12292–12303. Curran Associates, Inc., 2021.
- A. Schwartzman. Lognormal distributions and geometric averages of symmetric positive definite matrices. *International Statistical Review*, 84(3):456–486, 2016.

- L. Shao, Z. Lin, and F. Yao. Intrinsic riemannian functional data analysis for sparse longitudinal observations. *The Annals of Statistics*, 50(3):1696–1721, 2022.
- N. Tripuraneni, N. Flammarion, F. Bach, and M. I. Jordan. Averaging stochastic gradient descent on riemannian manifolds. In *Conference On Learning Theory*, pages 650–687. PMLR, 2018.
- O. Tuzel, F. Porikli, and P. Meer. Region covariance: A fast descriptor for detection and classification. In *Computer Vision – ECCV 2006*, pages 589–600. Springer Berlin Heidelberg, 2006.
- C.-H. Yang and B. C. Vemuri. Shrinkage estimation of the fréchet mean in lie groups. *arXiv:2009.13020*, 2020.
- J. Yang, R. Shi, and B. Ni. Medmnist classification decathlon: A lightweight autml benchmark for medical image analysis. In *2021 IEEE 18th International Symposium on Biomedical Imaging (ISBI)*, pages 191–195, 2021a.
- J. Yang, R. Shi, D. Wei, Z. Liu, L. Zhao, B. Ke, H. Pfister, and B. Ni. Medmnist v2 - a large-scale lightweight benchmark for 2d and 3d biomedical image classification. *Scientific Data*, 10, 2021b.
- Q. Zhang, L. Xue, and B. Li. Dimension reduction for fréchet regression. *Journal of the American Statistical Association*, 119(548):2733–2747, 2024.